

Design and development of an automated all-terrain wheeled robot

Debesh Pradhan¹, Jishnu Sen² and Nirmal Baran Hui^{*3}

¹ Fluid Section & Piping Division, MECON Ltd., Ranchi, India

²Department of Environmental Control System & Life System, HAL, Bangalore, India

³Department of Mechanical Engineering, NIT Durgapur, West Bengal, India

(Received November 27, 2012, Revised August 6, 2013, Accepted September 7, 2013)

Abstract. Due to the rapid progress in the field of robotics, it is a high time to concentrate on the development of a robot that can manoeuvre in all type of landscapes, ascend and descend stairs and sloping surfaces autonomously. This paper presents details of a prototype robot which can navigate in very rough terrain, ascend and descend staircase as well as sloping surface and cross ditches. The robot is made up of six differentially steered wheels and some passive mechanism, making it suitable to cross long ditches and landscape undulation. Static stability of the developed robot have been carried out analytically and navigation capability of the robot is observed through simulation in different environment, separately. Description of embedded system of the robot has also been presented and experimental validation has been made along with some details on obstacle avoidance. Finally the limitations of the robot have been explored with their possible reasons.

Keywords: All Terrain Robot (ATR); passive compliance mechanism; static force analysis; embedded systems; automation; simulation; real experiments

1. Introduction

All-Terrain Robots (ATRs) are the category of mobile robots that are capable of showcasing excellent off-road performances. They are able to navigate across bumpy and rough terrains. They mainly have wheels or tracks for locomotion. ATRs have various link mechanisms in order to overcome various sized obstacles. It is always desirable that the ATRs will be autonomous, that is, it will sense its environment with the help of sensors and then will take further decision on its own, with the help of instructions. The goal of this work was to conceive and build a mobile robot which will be a wheeled rover having good off-road capabilities, good grip over undulating, rough terrain, variable size obstacle negotiation capability, staircase ascending and descending capability, ditch/crevasse crossing capability and generating stable motion in undulating surface.

Quite a large number of researchers tried to design some ATRs through computer simulations. However, development of real ones is limited. It may be due to the huge complexity involved in building them. The book of Genta (2012) is a pioneer one in this field. After a thorough patent search, one American patent (Patent No. 499392, 1991), is found in this context. Owner of this

*Corresponding author, Associate Professor, E-mail: nirmalhui@gmail.com

patent (Patent No. 499392, 1991) has presented the construction details, operation and working conditions of a six wheeled stair case climbing robot. The robot has the capability of carrying a suitable pay-load like camera, microphone, shot-gun etc., and all the drives are remotely controlled. However, this robot cannot negotiate ditches and holes. Estier et al. (2000) & Siegert et al., (2002) have developed a space rover, which is able to passively overcome steps of 1.5 times the wheel diameter. They have presented experimental results of staircase climbing under the influence of friction and have shown the movement of Centre of Gravity (CG) of the robot. Thueer (2006) made an attempt to evaluate the locomotion performance of the ATRs. They have made a static 2D approach, in which wheel torques were optimized by minimizing the friction. Later on, Thueer and Siegwart (2010), Reina and Fogila (2013) developed an approach for evaluating the mobility of all-terrain robots, where there exist three classical methods in this regard (torque, slip and friction-based mobility assessment). However, Thueer and Siegwart (2010) have presented a technique based on velocity constraint violation. It has been observed that velocity constraint violation technique provides the best result compared to other mobility assessment methods. Moreover, Lamon and Siegwart (2005) presented a method for the measurement of wheel-ground contact angle and a traction control strategy by minimizing slip in rough terrain. According to them, torque control is more advantageous than the speed control of wheeled robots. In this regard, there exist three important wheeled mobility systems Ellery (2005), which are, the wheeled rocker-bogie suspension system, a tracked system (as exemplified by the Nanokhod rover suitably scaled), the elastic loop mobility system (ELMS).

Going through the above literatures, it is clear that the development of an ATR is a difficult job. It is more complex, if the ATR needs to perform in an optimal sense from every angle. Therefore, optimization of the design is required while modelling the robot. Development of an autonomous ATR is the prime aim of this research. Few important points are to be noted regarding design of an ATR, these are mentioned below.

- (i) performance parameters of ATRs are difficult to clarify quantitatively, but are determined by the motor torques, slope, incidence of obstacles, and the surface traction on the soil,
- (ii) turning radius will depend on the geometry of the vehicle and nature of turning mode,

Lamon and Siegwart (2004) have worked on the minimization of slip, which they have achieved by maximizing the traction forces. The system of equations that they have derived is non-linear and a numerical method was implemented to solve them. However, they could not provide any concrete idea on how this simulation technique will be helpful while designing a robot. Thueer and Kerbs (2007) also developed a method for optimizing the wheel torques and tested on two different robots CRAB and RCL-E. Later on, Ray and Brande (2009) proposed an approach for estimating net traction force and resistive wheel torques for a suspension-less, differentially-steered wheeled robot moving on a rigid or deformable terrain. Alexander and Maddocks (1989) have represented the wheeled mobile robot as a planar rigid body having an arbitrary number of wheels and included both rolling as well as the slippage due to wheel incompatibility in their model. Tarokh and McDermott (2005) did the same for articulated rovers, namely Rocky 7. They have considered several forms of rover kinematics and the simulation of robot-terrain interaction was also carried out. The navigational capabilities of the robot were also compared against unsymmetrical wavy bumpy terrain and serpentine path.

For better manipulation capability, sensors must be incorporated within the mechanical structure of the ATRs. There exists a large variety of sensors. The main problem in installing a

sensor is data acquisition and interpretation. Thus, there is a necessity to utilize the proper sensor and develop an error-free mechanism to perceive the data received by that particular sensor. Moreover, ATRs must have one guiding mechanism so that it can negotiate obstacles. Jarvis (1996) developed an all-terrain intelligent autonomous vehicle with a GPS and some range finders. Nickels and DiCicco (2010) developed a vision guided manipulation system. They have tried to position an instrument on a planetary surface. Chin and Wang¹ (2001) modified the conventional Distance Transform (DT) method for outdoor navigation of a vision-guided AGV. Their main emphasis was to plan the movement of the robot while navigating among some obstacles. Later on, Guivant and Nebot (2002) presented an algorithm for real time Simultaneous Localization and Map Building (SLAM). The accuracy of the SLAM algorithm was investigated in relation to standard localization algorithms using Kalman filter technique. This is purely a mathematical technique and computational complexity is high. Amina and Tanoto (2009) used a vision-based GPS to get the global position of the robot.

The goal of this work was to conceive and build a mobile robot which will be a wheeled rover having good off-road capabilities, good grip over undulating, rough terrain, variable size obstacle negotiation capability, staircase ascending and descending capability, ditch/crevasse crossing capability and generating stable motion in undulating surface. Simulation works were carried on the designed robot. Various result data were collected, for its movement in a particular terrain. A prototype robot has been designed and developed, presentation of which and its test results are the subject of this article. Thus the two various data from the simulation and the experiment can be compared and verified. This gives an overview of the efficiency of the design and the performance of the robot. The robot is finally made computer controlled integrating an ultrasonic range finder sensor through Basic Stamp PIC micro controller. Motor driver ICs are used to control the power supply to the motors. The capabilities of the robot are tested, and we have tried to find out the maximum potential. Rest of the paper is structured as follows. In Section 2, mechanical details of the developed robot are described and static force analysis of the robot is presented. Embedded systems including a sensor are placed inside the robot to make it autonomous and computer controlled, details of these are presented in Section 3. The robot is initially simulated using design simulation software [DSWM 2008] and results related to this and real experiments are presented in Section 4. Finally, some concluding remarks are made and scope for future work is indicated in Section 5.

2. Development of the mechanical structure and static force analysis

In this section, description of the mechanical structure of the developed ATR is made and static force analysis is carried out to test the balance of the robot.

2.1 Mechanical structure

A photograph of the robot is shown in Fig. 1 and a 2D model of the robot is shown in Fig. 2 with various parts for better realization.

The developed robot consists of four mechanical systems, which are described below.

- (i) **Passive System:** Passive joints denoted by front pivot and rear pivot (refer to Fig. 2)



Fig. 1 Photograph showing prototype of the developed all-terrain robot

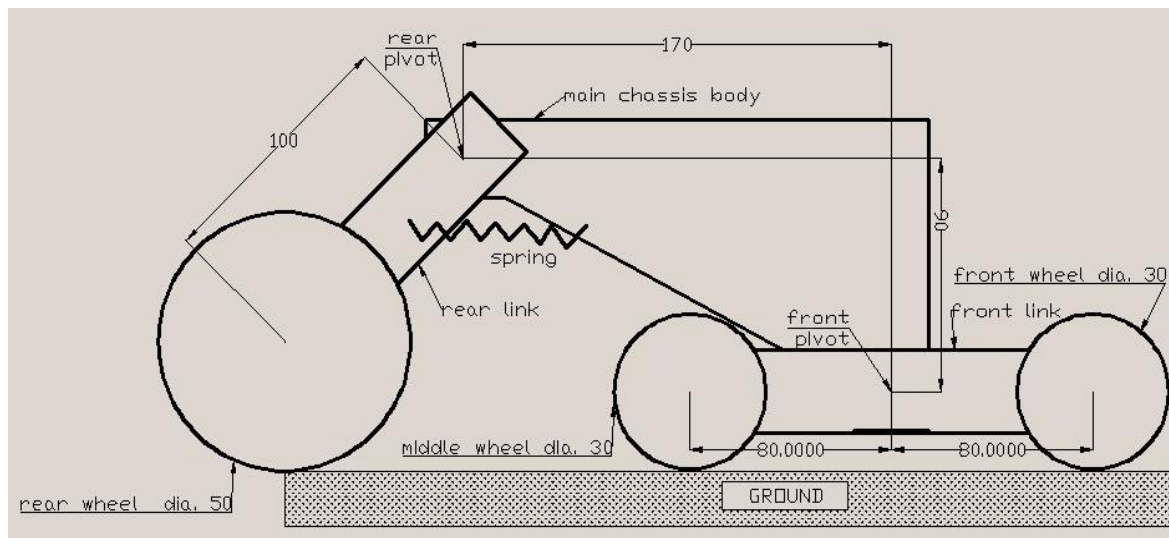


Fig. 2 A 2D (front view) mechanical drawing of the developed all-terrain robot

provides a passive compliance to the oncoming obstacles by rotating the links about the pivot. Hence, with the help of right and left half set of wheels (each set having 3 wheels), the ATR will normally have six point contact or a minimum of four point contact. This is because the front and middle wheels are not independent while the rear two wheels have independent sets of motion. This ensures maximum stability and adaptability as well as excellent climbing abilities. The weight of the whole robot, including payload, is well distributed over a larger area. The use of bearings in these joints ensures smooth operation

and reduces wear and tear. The friction between the surfaces is lessened, and the ball bearings carry some radial load. Thereby making the system more stable.

- (ii) **Connecting System:** This consists of the front links; the rear links and the spring (Refer to Fig 2). The front links not only connects the two motor wheel pair (i.e., the front and the middle wheels) but also gets attached to the main chassis by means of front pivot. Hence, this link can rotate about the front pivot and rear links can rotate about rear pivot. To restrain the motion of the rear links, they are connected to the chassis via spring of suitable spring constant. The springs used are helical compression springs. As a result of which, chassis will remain parallel to the ground under the application of load, and also it can allow some rotary motion of the links to negotiate obstacles. At the same time preventing the chassis to collapse under load by pulling the rear links with wheels attached and makes the robot successful in overcoming obstacles and stairs. The spring constant of rear springs are 40N/mm.
- (iii) **The Chassis:** It is made of aluminium sheet with frames and supports to prevent bending under loads. Aluminium usage reduces the weight of the frame, and at the same time adds to its strength. The chassis will house the payload and the electronic components for the operation of the rover. To prevent bending deformation under the load, supportive structures are incorporated along the sides. These aluminium angles strengthened the overall frame and also increases its load carrying capacity. Most importantly it prevents buckling, which is highly unwanted. Fasteners include nuts and bolts, rivets and screws.
- (iv) **Steering:** Differential type of steering is used. Hence the steering is simply achieved by rotating the left and right half set of wheels in the reverse directions. Thus each half (containing a set of rear, middle and front wheels) are controlled independently. This type of steering is called skid steering, like the ones employed in military tanks. Suppose the robot has to move by 90° , then the two sets of motors (left side and right side) turn in opposite direction. For example, if the robot has to move right, then the right side wheels turn in the backward direction while the left set of wheels turn in the forward direction. This turns the whole rover to right about a point, which is the centroidal axis. This minimizes the turning radius, making it as small as possible. The motors used are 12V 100 rpm 10Kg-cm DC motor. The rear wheels are slightly larger in diameter to keep proper contact with ground as and when front and middle wheels climb the step. The important dimensions (in mm) of the robot are shown in Fig. 2.

A slight modification in the rover can also be made by attaching a spring between the front link and the chassis as shown in Fig. 3. The model shown in Fig. 2 is termed as Rover 1 and the model shown in Fig. 3 is termed as Rover 2 for our future analysis purposes. Use of the additional spring in Rover 2 can be justified as the spring gets compressed when the front wheels encounter an obstacle, which helps to increase the normal reaction hence reduces slip. It becomes very much necessary to compare the designed rover with other passive systems so far developed. One of them is 'Shrimp (Estier et al. 2000)', comparison between Shrimp and Rover 2 is presented in Table 1.

2.2 Static force analysis

Let the masses of various components are denoted by:

- i. Mass of a front or middle wheel $(M_{fw}) = 0.056$ kg,

Table 1: Comparison between Shrimp and Rover 2

SHRIMP	Rover 2
It can climb almost twice its wheel dia.	It can also climb almost twice its wheel dia.
Bi-laterally symmetric	Bi-laterally symmetric
Differential steering.	Differential steering.
Size of all wheels equal.	Size of rear wheels larger than middle and front.
Contains large number of pivoted joints and links, thus increasing complexity.	Contains only four pivoted joints and links, thus simpler mechanical structure.
Can climb inclined plane up to 40°	Can climb inclined plane upto 37°
Lateral stability in rough terrain provided by two wheels on each side.	Lateral stability in rough terrain provided by three wheels on each side, hence more stable.
Use of spring in the front side to store energy once the first wheel has climbed the stair.	Use of front spring to increase normal reaction while climbing stair.
No rear springs.	Use of rear springs to produce more flexibility.

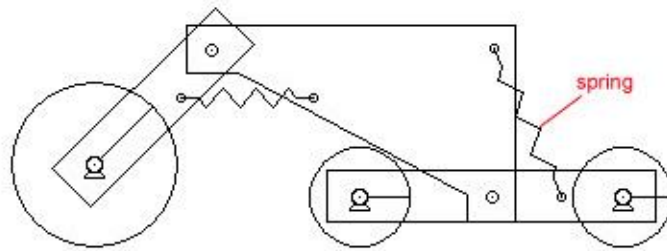


Fig. 3 A schematic 2D sketch of Rover 2, modified model of the Rover 1

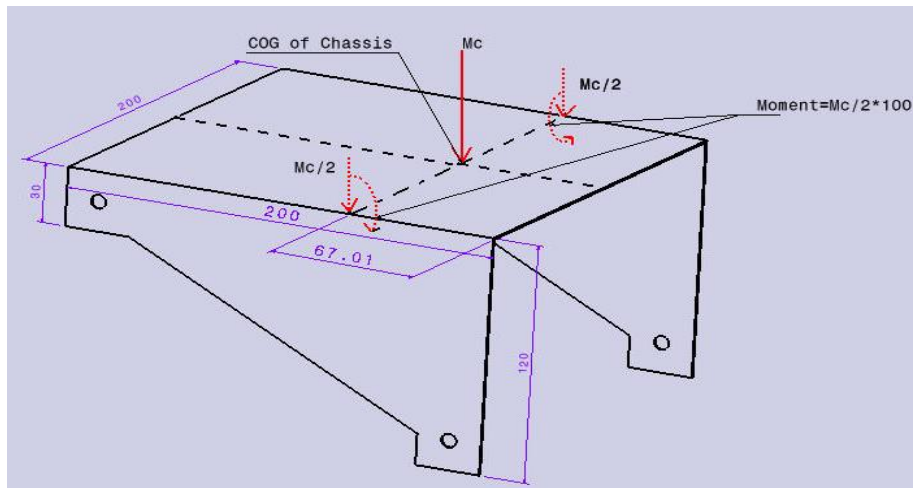


Fig. 4 A schematic figure showing the forces and torques acting on the chassis of the robot

- ii. Mass of each rear wheel $(M_{rw}) = 0.104$ kg,
- iii. Mass of each motor $(M_m) = 0.156$ kg,
- iv. Mass of rear link $(M_{rl}) = 0.064$ kg,

- v. Mass of front links $(M_{fl}) = 0.082 \text{ kg}$,
- vi. Mass of chassis + payload $(M_c) = 4.00 \text{ kg}$.

It is necessary to carry out the stability analysis of the said robot. Since, it is easy to perform the static force analyses in a 2D plane, hence, 3D weight system has been converted to 2D. Consider only the chassis, as shown in Fig. 4, with the payload acting at centre of mass of the chassis. Thereafter, the mass of chassis and payload (M_c) has been transferred to the sides shown by dotted arrows resulting in pair of bending moment and force $(M_c/2)*100$ and $M_c/2$, respectively. Now, the 2D static analyses for either left or right part of rover can be carried out as shown in Fig. 5, since it is bilaterally symmetric. Refer to Fig. 5, the solid arrow lines represent the actual weight of each component and the dotted line arrow on top represent total transferred mass. It is to be noted that that in this study, the centre of mass of rear link is at 25mm from rear pivot and not at middle as there is an extra mass of bearing coupled with link at rear pivot.

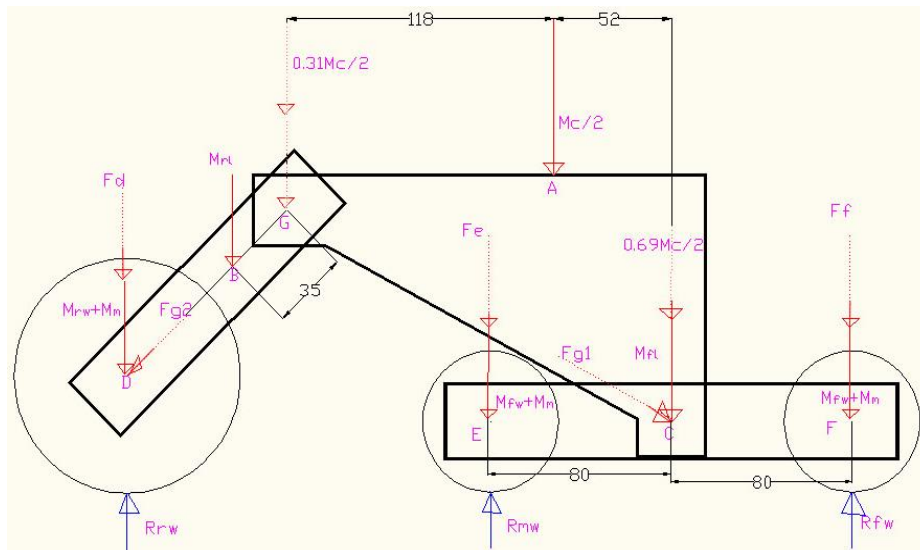


Fig. 5 Reaction forces, moments and torques acting on the robot

- The weight of payload and chassis on left half is $M_c/2$ acting at A (i.e., at the centre of mass of chassis). This has been transferred to rear pivot G given by $0.31 * M_c/2$ and the front pivot C given by $0.69 * M_c/2$.
- The weight of rear link M_{rl} has been transferred to pivot G given by $0.75 M_{rl}$ and rear wheel centre D given by $F_d = 0.25 M_{rl}$.
- The total load at G ($0.75 M_{rl} + 0.155 M_c$) is then transferred to rear wheel centre D given by $F_{g2} = (0.75 M_{rl} + 0.155 M_c) \cos(45^\circ)$ and front pivot C given by $F_{g1} = (0.75 M_{rl} + 0.155 M_c) \cos(55^\circ)$.
- Therefore, the total load at D is $= M_{rw} + M_m + F_d + F_{g2} \cos(45^\circ)$, which is also the reaction at back wheel.
- Again, total load at C is equally shared by wheel centre of front and middle wheel at F and

E, respectively. Analytically it can be calculated making equal to $M_m + M_{fw} + F_c = M_m + M_{fw} + M_{fl} + (0.96M_c/2) + (F_{gl} \cos(55^\circ))$.

Hence, this is the ground reaction on each of front and middle wheels.

2.3 Design basis for use of springs and link connecting the middle and front wheels

There are two springs namely front and rear springs. The rear springs connect the rear link with chassis allowing some flexibility which would be absent if instead rigid links was used. However, the use of front springs and the pivoted front link between middle and front wheels needs some further explanation.

The Fig. 6 shows that the Rover 2 is just about to climb the stair when the normal reaction on the front wheel from the horizontal ground is 0.

In absence of springs, the normal reaction from the vertical face of stair on the front wheels R_{vf} would be equal to total traction force due to rear and middle wheels.

Let the traction force on the pair of middle wheel be F_{tm} and that on rear be F_{tr} . Therefore, Normal reaction on set of middle wheels (refer to Section 2.2) will be

$$R_{mw} = [M_m + M_{fw} + M_{fl} + (0.96M_c/2) + (F_{gl} \cos(55^\circ))]g = 1.739 \times 9.81 = 17.06N.$$

Normal reaction on set of rear wheels will be equal to $R_{rw} = 0.37 \times 9.81 = 3.63N$.

Now, in presence of front springs, the normal reaction from the vertical face of stair on the front wheels R_{vf} = total traction force due to rear and middle wheels + (deflection of spring multiplied by the spring constant).

$$R_{vf} = F_{tm} + F_{tr} + \Delta.K \text{ where } \Delta \text{ is the deflection and } K \text{ is the spring constant.}$$

Also when the front wheel just raises from ground against the vertical face of stair, total mechanical load on front wheel = $R_{fw} = R_{mw} = 17.39N$ (See 2.2, Total load on front and middle wheels are equal).

Now, the condition for front wheel to lift from ground is:

Net traction force provided by vertical face of stair must be greater than the total mechanical load on front wheel at that instant, i.e., $\mu \times R_{vf} > R_{fw}$,

$$\Rightarrow \mu(F_{tm} + F_{tr} + \Delta.K) > R_{fw} \quad \Rightarrow \mu((\mu R_{mw}) + (\mu R_{rw}) + \Delta K) > R_{fw}$$

$$\text{i.e. } 0.7 \times ((0.7 \times 17.06) + (0.7 \times 3.63) + \Delta.K) > 17.39 \Rightarrow 14.48 + \Delta K > 24.84 \Rightarrow \Delta K > 10.46 N$$

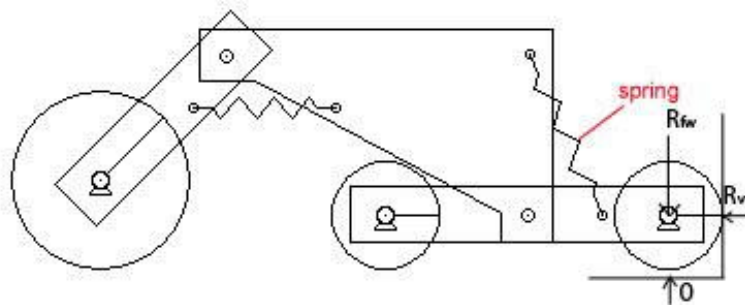


Fig. 6 Rover 2 negotiating a step obstacle

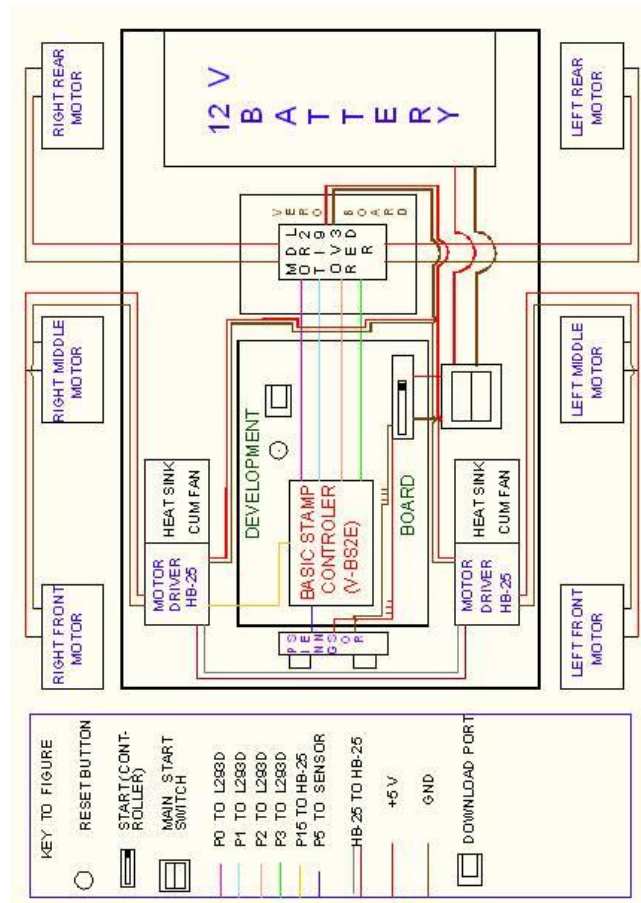


Fig. 7 A schematic layout showing the instrumentation of the manufactured robot

Now, the most probable domain for values of Δ varies between 1 mm to 5mm. On finding the range of K values for such a domain of Δ and using the values in simulation to get the smooth motion of rover we approach to a value of 4N/mm as the spring constant.

From above it is clear that use of front spring increases normal reaction against the vertical face of stair which aids in climbing the stair. As the front wheel gets raised the spring gets compressed however the middle wheel remains in ground since the link joining front and middle wheels is pivoted in the middle and free to rotate as per compression of front springs. This clearly explains use of front spring and link between middle and front wheels. Further, if the latter was a rigid joint and not pivoted in the middle the middle wheel would be found floating in air without any use during movement in staircase and other step obstacle overcoming.

3. Development of embedded system

Keeping in view that the developed robot is a proto-type and an experimental robot, the first step towards its automation is a basic controller circuit. By basic controller circuit we mean it

should have a microcontroller for storing the program of the task intended by the developer and processing the data from sensors and directing the actuators according to the sensed information.

In the developed All Terrain Automated Vehicle (AATV), the layout of the instrumentation is quite simple. The sensor that has been used is an ultra sound sensor that can detect obstacles in front of it. This sensor is connected to the pin no. 5 of the microcontroller (refer to Fig. 6), namely basic stamp version bs2e. There are two sets of motor drivers used such as HB-25 and L293d. There are two sets of HB-25 used again, one for each pair of left middle and front motors and other for a pair of right middle and front motors. Only one signal from the microcontroller is sufficient to control both the HB-25 motor drivers and it is made through pin no. 15 of the microcontroller (as shown in Fig. 7).

The other motor driver being the L293d IC has two H-bridge circuit within it. It is used to control the rear end motors. Hence it can control two DC motors at a time. Architecture of H-bridge is such that it needs two control signals, which it is receiving through four IO lines (pin no. 0 to 3 via resistance for protection of the IC) from micro-controller (refer to Fig. 7).

The battery is connected initially to the main start switch, from where supply branches out to three, i) L293d IC, ii) HB-25 DC motor controller and iii) the development board. The development board has on board 5V converter that extracts 5V from the battery and sends it to the microcontroller and connectors. The sensor also takes its 5V supply and GND from those connectors in the development board. The development board has the reset switch, start switch and the port for downloading the program from the controller.

4. Results and discussions

Results include firstly the simulation carried out on a similar model. The simulation is carried out on an artificial environment, similar to planetary surfaces using Software working model 2D [18]. Graphical variations of position, velocity and acceleration with time are depicted from the simulation results. Also the environmental parameters are varied within a range, and the performance of the simulated prototype is judged, when made to negotiate with them. Following parameters of the robot and environment are varied during simulations.

- (i) stiffness of the spring,
- (ii) front wheel dimensions,
- (iii) rear wheel dimensions,
- (iv) location of the joint where the front wheel arm is attached to the main body,
- (v) prototype mass (including pay-load),
- (vi) front set of wheels to act as tracked wheels.
- (vii) roughness pattern of the terrain
- (viii) angle of inclination of the slope encountered.

Thereafter, experiments with the real robot were carried out to test the capability of the robot in tackling different terrain conditions.

4.1 Simulation results

Computer simulations have been conducted on both Rovers 1 and 2. Coefficient of friction

between the wheel and landscape is considered to be 0.7 both static and otherwise. It has been noticed that the Rover 1 was able to overcome an obstacle 1.5 times its front wheel diameter. On the other hand, Rover 2 was able to climb a step height, which is 2.5 times its wheel diameter. Movement of Rover 2, negotiating a step obstacle is shown in Fig. 8.

Performances of both the Rovers were also tested while moving on three different terrains (staircase, bumpy track and sloping surface) through computer simulation (refer to Figs. 9 and 10, respectively). Fig. 11 represents the linear 2D position (X and Y) of the CG of the robot, rotation, rotational speed and rotational acceleration of centre of mass of the front wheel of Rover 1 with time, while navigating in a terrain comprising of staircase, rocky landscape and sloping surface as

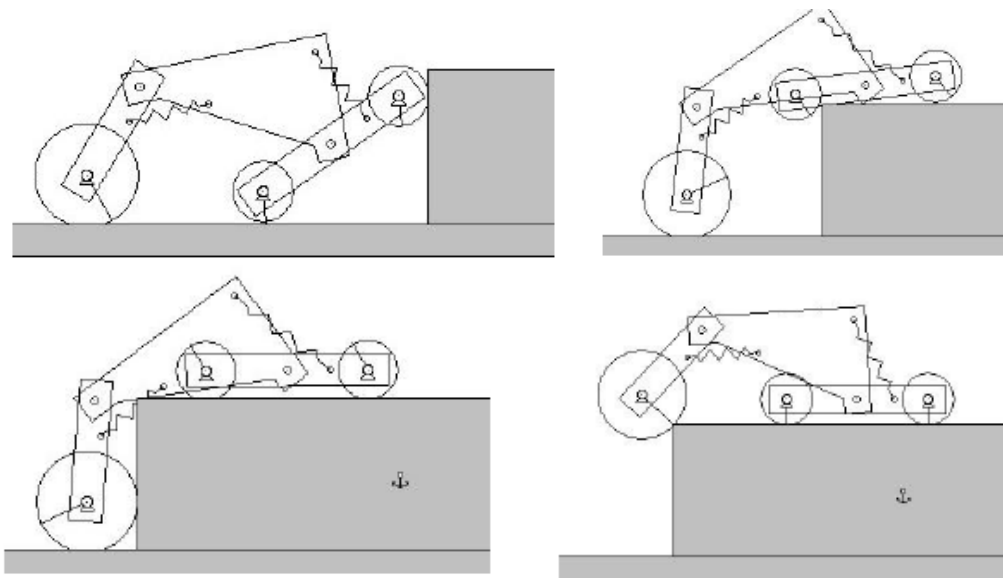


Fig. 8 Movement of Rover 2 negotiating a step obstacle

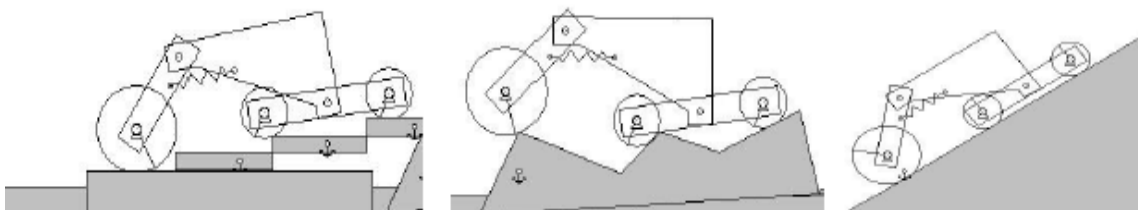


Fig. 9 Navigation of Rover 1 against three different terrains

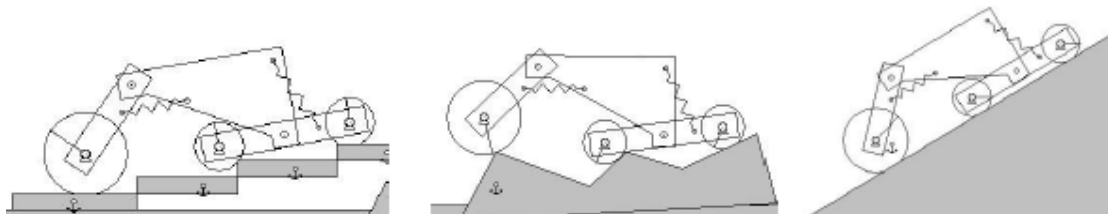


Fig. 10 Navigation of Rover 2 against three different terrains

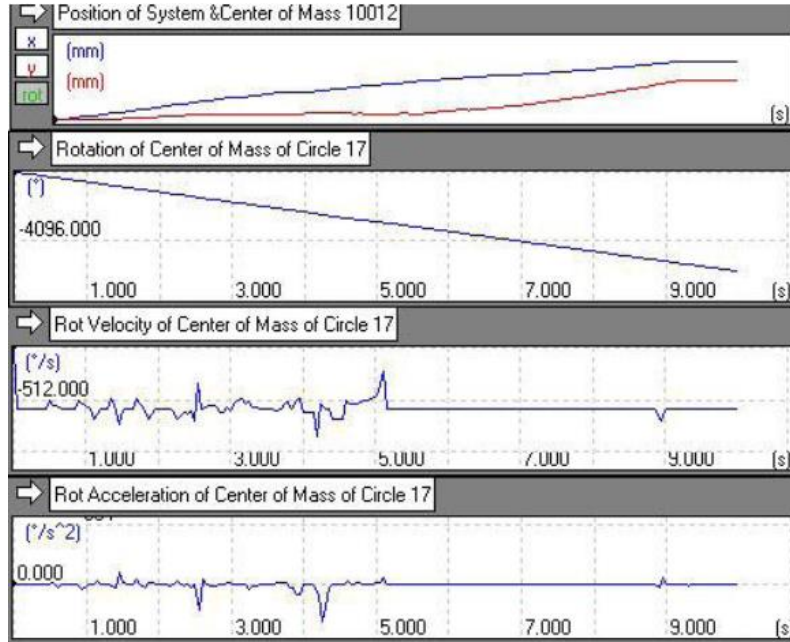


Fig. 11 Linear position of Robot's CG, rotation, rotational speed and acceleration of CG of front wheel for Rover 1

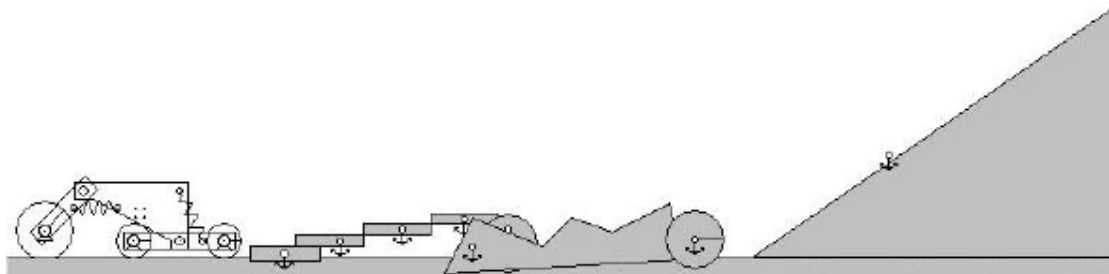


Fig. 12 A schematic figure showing the combination of different planetary surface

shown in Fig. 12. Similarly, movement of the Rover 2 is energized on the same environment as shown in Fig. 12. Fig. 13 represents the linear 2D position of the CG of the robot, rotation, rotational speed and rotational acceleration of centre of mass of the front wheel for Rover 2.

Both the Rovers were allowed to navigate on a road comprising of three different landscapes as shown in Fig. 12 for eight seconds. Out of the total eight seconds, for approximately the first two seconds rovers were allowed to ascend on stairs, next three seconds tentatively on uneven surface have some sharp peaks and last few seconds on a sloping surface having a slope of 37 degree approximately. Angular position, speed and acceleration of the front wheel of both the rovers at some discrete instants of time are noted and tabulated in Table 1. Going through the results obtained, following common observations are made.

- Through trial and error, the spring constants for the rovers are set to 40N/mm and 4N/mm for the back and front springs, respectively in the simulated models. The values higher than this make

the links stiff, bringing about an obstruction in the passive system. While with lower values of the same causes some unwanted vibratory motions of the links indicating unstable movement of the rovers.

- Size of the wheels is taken in proportion to the size of the rovers. Smaller diameter wheels will provide low performance, due to closeness to ground causing links to interfere with the obstacle. On the other hand, larger size wheels become disproportionate and bulky.
- Location of the front pivot is considered at the centre of the member connecting the front wheels. Little shift of this pivot point towards any one of the wheels might improve the navigation capability of the rovers among step obstacles. However, there will be a high risk of overturning of the wheels leading to loss of stability of the rover.
- With the increase in cart mass the simulation shows difficulty in overcoming step obstacles and tends to get stuck at some points in the bumpy terrain.
- It is important to note that the simulation shows that both the rovers get stuck more often in bumpy surfaces having sharp peaks. This can be avoided by placing the front pivot in a greater height and using a front link connecting the front wheels in the shape of an inverted-U rather than a straight and/or using track belt connecting the front and middle wheels of each left and right half. However, all those design modification increases the complexity in the model.
- While tackling step obstacles, Rover 1 requires more angular speed and acceleration than Rover 2 (refer to Table 1). It could be due to the fact that the presence of extra spring on Rover 2 reduces the traction force on the front wheels. Therefore, Rover 2 is more stable than Rover 1 while navigating among step obstacles.
- On a bumpy terrain, movement of Rover 2 has seen to be smoother and slower than the Rover 1. However, Rover 2 requires more torque on the front wheels while crossing sharp peaks and this additional torque might be used to store the energy on the front spring of Rover 2, which in turn will provide fewer jerks on the cart.
- During movement in an inclined plane, angular speed have come out to be constant (refer to Table 1). This is a common fact coming true. With the increase in slope, there is a chance of slippage of the robot. Angle of slope surface without slip the robots can handle is almost found to be same for both the rovers. However, increase or decrease in the torque generating capacity of the motors, friction between the tyre and terrain might provide different results in that respect.

4.2 Experimental validation

All the simulation results are futile unless a rover of similar climbing facilities is produced physically. Not only this but it should also match its performance similar to that in the simulation. For this very purpose, we have carried out many experiments and presented in this section. Test terrains that have close approximation to the simulation terrains were built to get a realistic definition of movement of the rover. Besides it is also notable that the real model and virtual model has the same defining parameters like – weight of each links, rpm of motor, weight and dimension of each wheels, spring constant of springs etc. The results presented here have been accompanied with images as proof. The various tests conducted include inclined plane climbing, stair case climbing, step/obstacle negotiation, obstacle detection and avoidance, ditch crossing etc. All of these have been described below and it is to be noted that all experiments are with Rover 2.

Table 1 Angular position, speed and acceleration of the front wheel of the rovers in different instant of time while navigating a terrain shown in Fig. 12

Landscape Condition	Time (Secs.)	Rotation (deg.)		Speed (deg/s)		Acceleration (deg/s ²)	
		Rover 1	Rover 2	Rover 1	Rover 2	Rover 1	Rover 2
Step Obstacle	1.15	681.79	681.94	656.51	648.23	-1742.90	1338.51
	1.45	859.30	855.86	743.50	574.61	-7008.58	947.95
	1.8	1065.59	1071.48	598.21	519.80	2024.00	-25.18
Irregular Surface	2.6	1564.43	1570.42	567.03	646.13	-60.19	-1480.82
	3	1797.60	1808.33	564.19	597.81	388.80	-611.35
	4	2389.58	2414.61	680.90	709.23	4883.35	-935.04
Inclined Plane	6	3565.00	3565.47	600.00	600.00	-10 ⁻⁷	-10 ⁻⁴
	7	4165.23	4165.47	600.00	600.00	-10 ⁻⁹	-10 ⁻¹¹
	8	4765.23	4765.47	600.00	600.00	-10 ⁻¹⁰	-10 ⁻¹¹

(a) $t = 4.5\text{sec}$ (b) $t = 5\text{sec}$ (c) $t = 6\text{sec}$ (d) $t = 7\text{sec}$

Fig. 14 Sequence of obstacle climbing of height equals to the diameter of the front wheels 6 cm

4.2.1 Steps/ obstacle climbing

The rover is easily able to climb a step height of 6 cm (equal to its front wheel diameter) (Fig. 14). The test terrain is made of ply and the coefficient of friction is less than 0.4 for plastic-plywood (painted) surface, whereas in simulation we used 0.7, still the robot is able to climb this

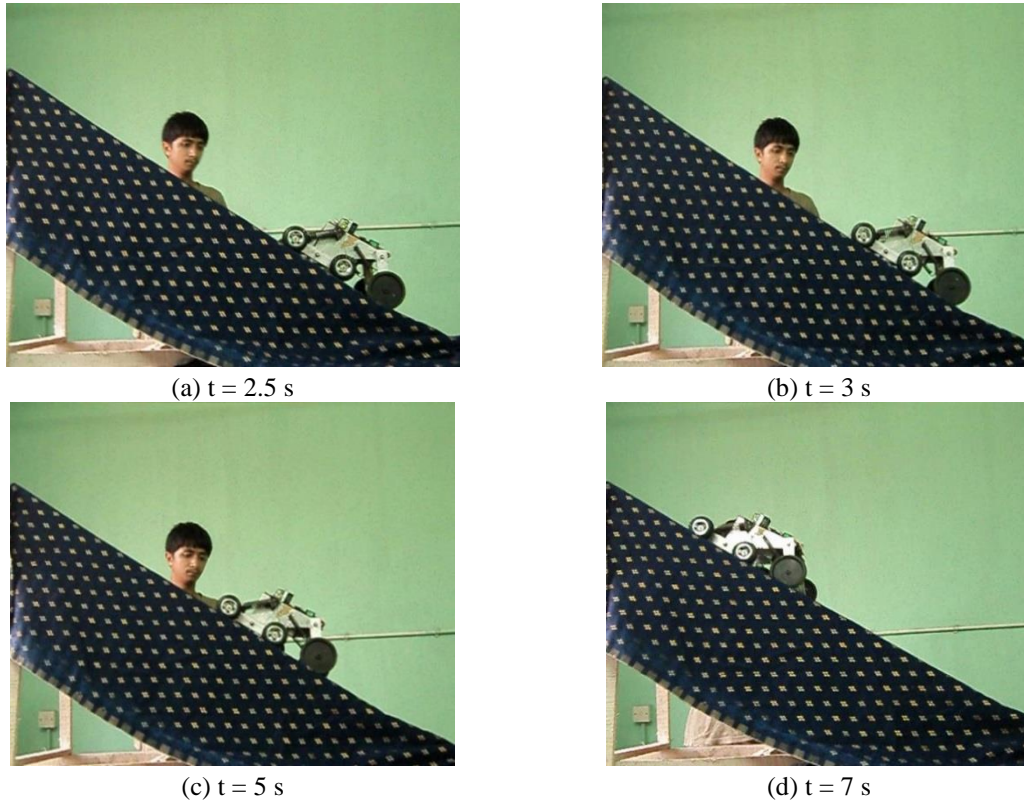


Fig. 15 Sequence of inclined planed climbing

height successfully. When we increased the step height to 12 cm the robot was not able to climb as the wheels were seen slipping. But in simulation we have found that it is able to climb this much of height. The problem here is due to less coefficient of friction, which is only 0.4 in this case. However, during simulation as mentioned before, the coefficient of friction is taken to be 0.7. Now, we decreased the step height to 9 cm and slightly increased the friction coefficient by placing a cloth/canvas. This time the robot was able to overcome the obstacle.

4.2.2 Inclined plane climbing

In the simulation the rover is able to climb maximum of 37° , when the coefficient of friction is 0.7. In real experiments as shown in Fig. 15 below it was found that the rover was able to climb maximum of 36° . The close resemblances of the results indicate the similarity between the real model and the virtual model built for simulation.

4.2.3 Staircase ascending

The sequence of staircase ascending has been shown in the Fig. 16. The height of the step is 4cm that is slightly less than front wheel size and length of step is 200cm. It was found similar to our simulation; the rover could tackle these steps without any difficulty. However, it is to be mentioned that the rover with front springs removed was unable to climb these steps as it was seen that the front links were getting stuck. This clearly justifies the use of those springs.

(a) $t = 1$ s(b) $t = 2$ s(c) $t = 3$ s(d) $t = 3.5$ s(e) $t = 4$ s(f) $t = 9$ s(g) $t = 9.5$ s(h) $t = 10$ s

Fig. 16 Sequence of staircase ascending

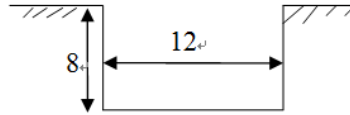


Fig. 17 Test ditch

4.2.4 Ditch crossing and deformable surface

The rover was successful in crossing a test ditch of depth 8 cm and width 12 cm which has been shown in Fig. 17. As for the deformable terrain the testing was done on a grassy ground with grass height up to 10 cm. The rover could easily move through even such a surface.

4.3 Comparison with existing rovers

The rover described in this paper uses passive compliance mechanism to negotiate obstacle. This is an advantage against rovers where each joint is separately controlled (King *et al.* 1991), which requires complex control system and circuitry to control each joints as well as wheel motors.

Now, if we compare this rover with existing rovers with passive compliance, the best among those that already exists is the Solero or Shrimp robot (Estier *et al.* 2000). This has the climbing ability of steps which are almost more than 2 times its wheel size. The rover presented in this paper is a modification of Rocker Bogie (RE) type model. Even though normal rocker bogie (RE) rovers do not have high climbing abilities like Solero, Rover 2 presented out here has same climbing abilities like Solero. But what is notable out here is that these climbing abilities are achieved without using complex parallelogram configuration or parallel suspension architectures as in case of Solero. This has been achieved by the use of springs, location and number of passive joints and changes in size of wheels.

We find that in case of Shrimp/Solero the loads are not evenly distributed in the wheels, hence we find high peaks in torque diagram for the back wheels showing strongly unbalanced load when the rover climbs steps (Thueer *et al.* 2006). Even other rovers like Crap and RCL have the same problem (Lamon and Siegart 2005).

The rover presented has more even load distribution. When the rover encounters a step obstacle at first the back wheel torque peaks even in this case but unlike other rover it is smooth when other two sets (i.e. rear and back) wheels climb the step. This result was obtained when the spring constant for rear spring was taken to be 35 N/mm (springs used by the rover manufactured in the laboratory). It was found in simulation that with the decrease in the spring stiffness the compliance between the rover chassis and back wheel increased and the torque peak for rear wheel decreases. But all of these come at the cost of increase in vibration and decrease in payload capability. Hence these needs to be optimized and are under investigation. Hence, the developed rover has got excellent climbing abilities with a simple configuration and cost effective.

5. Conclusions

Demand for the development of a single robot, which can negotiate staircase, slope surface, bumpy track is increasing day-by-day. Scientists at NASA are working in this line for quite some time. Many other researchers have also tried to design and/or develop the same. Variety of complex

research problems are involved in developing the same and a large number of researchers across the World are working in this field. One such basic problem is to design and develop a suitable mechanical structure.

In the present study, an attempt has been made in this regard. Two different kind of mechanical structures, namely Rover 1 and Rover 2 have been designed and tested through computer simulations initially. Both the rovers consist of six differentially steered wheels (four at the front and two at the back of the cart). They are pivoted with the cart through a member, so that one additional degree of freedom is generated and is then acting as a compliance mechanism. A spring is attached with the member connecting the back wheels and the cart so as to prevent the overturning of this member while encountering step obstacles. Presence of another spring in front side has been considered for Rover 2 for smooth operation of the robot. Performances of both the Rovers have been tested through computer simulations using the software (DSWM 2008) while they are navigating across a staircase, bumpy terrain and slope surface. Rover 2 has been observed to perform well across staircase and slope surface. On the other hand, Rover 1 has crossed the bumpy terrain with more speed. This difference in performance has occurred due to the presence of the front spring in Rover 2. Finally, a prototype model of the Rover 1 has been manufactured and its performance was tested while navigating among step obstacles. It has been observed that the developed robot was very easily tackling step heights up to 1.5 times its front wheel diameter.

The designed and developed robot will be helpful to tackle all the three kind of terrains discussed in the paper, thus, making it suitable for planetary explorations. Developed robots have limitations due to its mechanical structure. It can be improved in many ways. The wheels can also be connected with the cart in some other way too. Moreover, presently the robot is having only one sonar sensor. One camera can be placed and may be used to take snap-shots at different locations. Also the controller program is compiled initially in the computer and then downloaded to real Rover. It will be more interesting, if it is controlled through a processor placed at a distant apart from the Rover. The authors are working towards these issues presently.

References

- Alexander, J.C. and Maddocks, J.H. (1989), "On the kinematics of wheeled mobile robots", *Int. J. Robotics Res.*, **8**(5), 15-27.
- Amina, S., Tanoto, A., Witkowskia, U., Rückert, U. and Abdel-Wahabb, M.S. (2009), "Effect of global position information in unknown world exploration - a case study using the teleworkbench", *Robot. Auton. Syst.*, **57**(10), 1042-1047.
- Chin, Y.T., Wang, H., Tay, L.P., Wang, H. and Soh, W.Y.C. (2001), "Vision guided AGV using distance transform", *Proc. of the 32nd Intl. Symp. On Robotics*, 19-21 April.
- Design-Simulation, Working Model 2D (DSWM) (2008), URL: [http:// www.designsimulation.com/WM2D](http://www.designsimulation.com/WM2D).
- Ellery, A. (2005), "Environment-robot interaction - the basis for mobility in planetary microrovers", *Robot. Auton. Syst.*, **51**, 29-39.
- Estier, T., Crausaz, Y., Merminod, B., Laurai, M., Piguët, R. and Siegwart, R. (2000), "An innovative space rover with extended climbing abilities", *Proc. of the Fourth Intl. Conf. and Exposition on Robotics for Challenging Situations and Environments*, Albuquerque, NM, 333-339.
- Estier, T., Piguët, R., Eichhorn, R. and Siegwart, R. (2000), "Shrimp: a rover architecture for long range Martian mission", The Netherlands, December 5-7.
- Siegwart, R., Lamon, P., Estier, T., Lauria, M. and Piguët, R. (2002), "Innovative design for wheeled locomotion in rough terrain", *Robot. Auton. Syst.*, **40**(2-3), 151-162.
- Genta G. (2012), *Introduction to the Mechanics of Space robots*, Springer Verlag, **26**, Netherlands.

- Guivant, J., Nebot, E. and Whyte, H.D. (2002), "Simultaneous localization and map building using natural features in outdoor environments", *Robot. Auton. Syst.*, **40**(2-3), 79-90.
- Jarvis, R. (1996), "An all-terrain intelligent autonomous vehicle with sensor-fusion-based navigation capabilities", *Control Eng. Pract.*, **4**(4), 481-486.
- King, E.G., Shakelord, Jr. H.H. and Kahl, L.M. (1991), "Staircase climbing robot", *United States patent, patent no.4993912*, Date of Patent: Feb. 19.
- Lamon, P., Siegwart, R., Thueer, T. and Jordi, R. (2004), "Modelling and optimization of wheeled robots", *Proc. of the 8th ESA Workshop on Advanced Space Technologies for Robotics and Automation*.
- Lamon, P. and Siegwart, R. (2005), "Wheel torque control in rough terrain—modelling and simulation", *Proc. Of IEEE Intl. Conf. on Robotics and Autonomous Systems*, Barcelona, Spain, 867- 872.
- Nickels, K., DiCicco, M., Bajracharya, M. and Backes, P. (2010), "Vision guided manipulation for planetary robotics - position control", *Robot. Auton. Syst.*, **58**(1), 121-129.
- Ray, L.R., Brande, D.C. and Lever, J.H. (2009), "Estimation of net traction for differential—steered wheeled robots", *J. Terramechanics*, **46**, 75-87.
- Reina and Fogila (2013), "On the mobility of all-terrain rovers", *Ind. Robot.*, **40**(2), 121-131.
- Tarokh, M. and McDermott, G.J. (2005), "Kinematics modeling and analyses of articulated rovers", *IEEE T. Robot.*, **21**(4), 539-553.
- Thueer, T., Kerbs, A. and Siegwart, R. (2006), "Comprehensive locomotion performance evaluation of all terrain robots", *Proc. of IEEE Intl. Conf. on Intelligent, Robots and Systems*, 4260-4265.
- Thueer, T., Kerbs, A., Siegwart, R. and Lamon, P. (2007), "Performance comparison of rough-terrain robots -simulation and hardware", *J. Field Robot.*, **24**(3), 251-271.
- Thueer, T. and Siegwart, R. (2010), "Mobility evaluation of wheeled all-terrain robots", *Robot. Auton. Syst.*, **58**, 508-519.